PERGAMON

Chemical Engineering Science 56 (2001) 2685–2693

Chemical Engineering Science

www.elsevier.nl/locate/ces

Preparation of silicon-carbide-coated activated carbon using a high-temperature fluidized bed reactor

J. E. Atwater[a,*], J. R. Akse[a], T.-C. Wang[a,1], S. Kimura[b], D. C. Johnson[c]

[a]*UMPQUA Research Company, P.O. Box 609, 125 Volunteer Way, Myrtle Creek, OR 97457, USA*
[b]*Chemical Engineering Department, Oregon State University, Corvallis, OR 97331, USA*
[c]*Materials Science Institute and Department of Chemistry, University of Oregon, Eugene, OR 97403, USA*

Received 24 March 2000; received in revised form 9 October 2000; accepted 17 October 2000

Abstract

Chemically and thermally stable high surface area catalyst supports are needed to facilitate a vast array of chemical reactions. One approach is to augment an otherwise vulnerable high surface area material such as activated carbon with a robust surface coating. Here a high-temperature fluidized bed reactor-based method for the production of silicon-carbide-(SiC) coated activated carbon is described. At 1350°C, gaseous silicon monoxide reacts at the carbon surface to form β-SiC and carbon monoxide. The resulting carbide coating confers improved resistance to thermal and chemical degradation while maintaining significantly high surface areas. The resulting composite materials are characterized by scanning electron microscopy, X-ray diffraction, X-ray fluorescence, electron microprobe, BET surface area, and thermogravimetric analysis.

Keywords: Fluidization; Imaging; Materials; Processing; Reaction engineering

1. Introduction

One of the most attractive features of activated carbon as a catalyst support is that forms are available with relatively high surface area ($\approx 2000\ m^2/g$) as compared to more traditional ceramic support materials (20–250 m^2/g). Workers in our laboratory have exploited this property in the preparation of extremely active carbon-supported bimetallic noble metal catalysts for the deep oxidation of aqueous organics (Akse, Atwater, McKinnis, Thompson, & Hurley, 1997; Atwater, Akse, McKinnis, & Thompson, 1997a; Atwater, Akse, McKinnis, & Thompson, 1996; Akse, Thompson, Scott, Jolly, & Carter, 1992; Akse & Jolly, 1991). Using these catalysts the complete destruction of typical aqueous contaminants such as alcohols, ketones, organic acids, phenols, aromatics, halocarbons, and jet fuel, has been demonstrated under substantially milder reactor operating conditions than are possible using more conventional catalyst preparations. A significant limitation of current carbon-supported catalysts is that they are mechanically weak and therefore are susceptible to attrition if the momentum transport is large for the particular process. In the case of carbon-supported noble metal catalysts used for aqueous-phase oxidations, the loss of fine particles resulting from mechanical effects can be extremely costly. Carbon- supported catalysts are also susceptible to oxidation. The desirability of an alternative catalyst support has been suggested in many studies (Akse et al., 1997; Sharma, Zhou, Tong, & Chuang, 1995; Parmaliana, Alekseev, Nesterov, Ryndin, & Giordano, 1986; Bruno et al., 1983).

Ledoux, Hantzer, Cuong, Guille, and Desaneaux (1988), Ledoux, Guille, Hantzer, and Dubots (1990) and Cuong et al. (1994) have found the use of silicon carbide (SiC) as a catalytic support advantageous in high-temperature gas-phase catalytic reactions, because SiC is highly stable from thermal, chemical and mechanical perspectives. These workers attempted to prepare a SiC-coated monolith with a specific surface area equivalent to that of activated carbon by wash coating activated carbon onto a ceramic honeycomb and then reacting the carbon with gaseous silicon monoxide (SiO) at temperatures between 1100 and 1400°C, and pressures between 0.1 and 1 Torr. However, the morphology of the product

* Corresponding author. Tel.: +1-541-863-7770; fax: +1-541-863-7775.

E-mail address: jatwater@engr.orst.edu (J. E. Atwater).

[1] Current address: WaferTech LLC, 5509 N.W. Parker St., Camas, WA 98607, USA.

0009-2509/01/$ - see front matter
PII: S0009-2509(00)00515-7

SiC was significantly different from that of the original activated carbon. Reduced surface area of the SiC support resulted in catalysts with much lower activities. Moene, Kramer, Schoonman, Makkee, and Moulijn (1997) and Moene, Makkee, and Moulijn (1998) utilized a fluidized bed reactor to produce a SiC catalyst support by reacting gas-phase hydrogen and silicon tetrachloride with nickel-impregnated activated carbon. This work produced material with surface areas ranging between 25 and 80 m^2/g.

For the purposes of preparing a more effective catalyst support, bulk conversion of the carbon to silicon carbide may be counterproductive, since the silicon carbide forms a crystalline structure which results in substantially reduced surface area. For this reason, we chose to explore the means for the production of a thin outer coating of SiC to protect the underlying carbon from attack by chemical, thermal, and mechanical means. Preliminary experiments conducted in a tube furnace demonstrated the production of a SiC-coated activated carbon (SiC/C) but also indicated considerable difficulty in obtaining uniformity of SiC deposition (Atwater et al., 1997b). Recently, fluidized-bed reactors have been widely applied to chemical vapor deposition (CVD) processes for the modification of powder surfaces, such as composite particles and surface coatings (Kage, Yoshida, Ogura, & Matsuno, 1996; Morooka, Okubo, & Kusakabe, 1990). Fluidization conditions may facilitate the production of a homogeneous surface coating via rapid mixing of solids and high-mass transfer rates (Kunii & Levenspiel, 1991; Levenspiel, 1972). Hence, it was anticipated that the gas–solid reaction of activated carbon and SiO vapor in a high-temperature fluidized-bed reactor could be utilized for the efficient production of SiC/C particles, with desirable characteristics in terms of quality and uniformity.

To this end, reactions were conducted in a high-temperature fluidized-bed reactor (HTFBR). The reactor was first charged with activated carbon, preheated with an argon–hydrogen mixture to remove adsorbed gases from the surface of the granular media, then charged with solid SiO, and fluidized using the argon–hydrogen carrier gas. Reaction temperatures ranging between 1200 and 1350°C were investigated. The physical characteristics of the resulting SiC/C were characterized using BET surface area, X-ray diffraction (XRD), scanning electron microscopy (SEM), electron probe microanalysis (EPMA), and thermogravimetry (TGA).

2. Experimental section

2.1. High-temperature fluidized-bed reactor (HTFBR) design and operation

The reactor used in this study is illustrated schematically in Fig. 1. The HTFBR system has been described in detail elsewhere (Jovanovic, Kimura, & Levenspiel, 1994). The reactor consists of a 55 mm (ID) × 1200 mm (L) alumina tube and distributor plate mounted inside a vertically oriented tube furnace with a 100 mm (ID) × 1500 mm (L) tube, and an upper temperature limit of 1600°C. The reactor is designed to produce the fluidized bed in the center zone of the furnace where the most uniform temperature occurs. The reactor is augmented by systems for the control of carrier gas and gaseous reactants, and by a pneumatic system for the delivery of solid reactants. The pneumatic system is also used for the removal of samples and for the discharge of product. Reactor temperatures are monitored using two thermocouples: one located inside the bed, and the second inserted into the plenum 1 cm below the distributor plate. Gases are delivered from cylinders through calibrated rotameters, and are adjusted using flow control valves. Inlet and outlet pressures, and reactor temperatures are monitored continuously using a computerized data acquisition system. Two types of flow distributor were used: a 0.5 cm perforated alumina disk, and a 2.5 cm porous alumina disk.

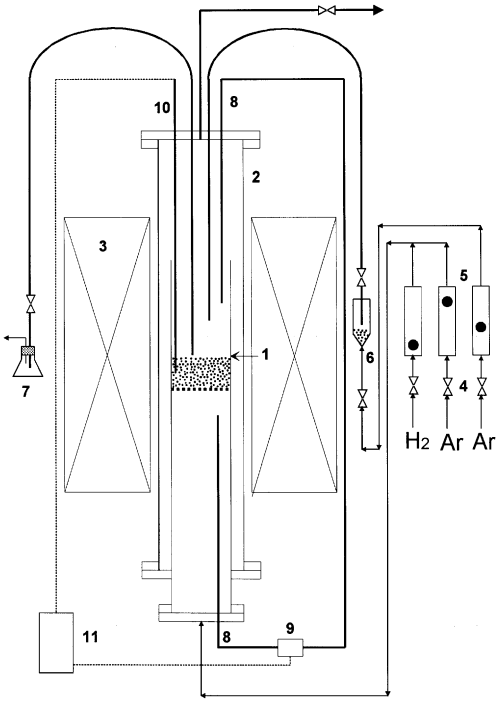

Fig. 1. High-temperature fluidized bed reactor (HTFBR) schematic: 1, fluidized-bed reactor; 2, furnace tube; 3, furnace; 4, control valve; 5, flowmeter; 6, pneumatic solid charger; 7, pneumatic solid discharger; 8, pressure probe; 9, pressure transducer; 10, thermocouple; 11. data acquisition system.

Minimum fluidization velocities were determined for the activated carbon substrate using both porous and perforated distributor plates from the relationship between the differential pressure and superficial fluid velocity using the argon carrier gas. These preliminary

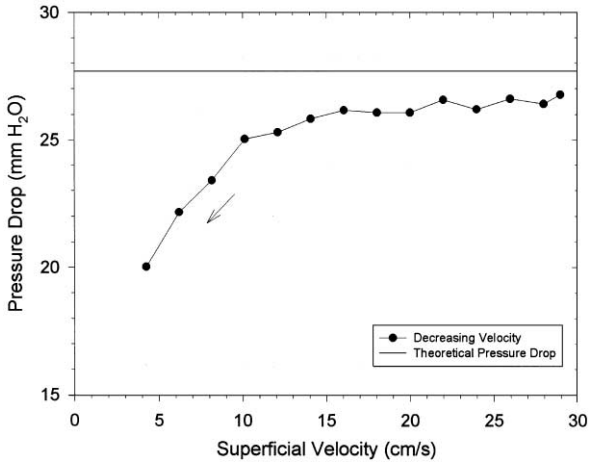

Fig. 2. Minimum fluidization velocity of activated carbon at 1350°C.

experiments were conducted at both ambient temperature and 1350°C. Differential pressures were monitored with both increasing and decreasing flow rates. Data gathered in the decreasing flow regime were used in the determination of minimal fluidization velocities. No significant differences were evident between ambient and elevated temperature for either distributor. As shown in Fig. 2, a minimum fluidization velocity of ~ 15 cm/s was determined for the activated carbon. In operation, the velocity of the argon carrier was, in general, set at two times the minimum fluidization velocity, to prevent the formation of dead zones.

Prior to each reactor run, activated carbon was introduced into the bed before insertion of the reactor tube into the furnace. The system was then heated to reaction temperature at a rate of 8°C/min, while the required flow rate of Ar gas was supplied continuously. After the temperature reached steady state, the composition of the carried gas was changed to 90% Ar and 10% H_2, by volume. Hydrogen was used to facilitate the removal of adsorbed oxygen from the carbon surface, to prevent the formation of undesirable oxide impurities. After 1 h of pretreatment, SiO was pneumatically introduced into the fluidized bed to initiate the reaction. Samples were periodically collected for analysis. After each run, the system was cooled to room temperature, the reactor tube was disassembled, and the remaining product was collected. The reactor was operated over a range of temperatures and reaction times. The rate of introduction of the SiO was also varied.

2.2. Catalyst preparation

Bimetallic platinum–ruthenium oxidation catalysts were prepared using both untreated activated carbon (Barnaby-Sutcliff 580-26) and SiC/C supports by the deposition of ruthenium and platinum salts, followed by thermal decomposition of the salts under reducing conditions. Details of the preparation of RP-121, the carbon-supported catalyst, have been reported elsewhere (Atwater et al., 1997, 1998). A 5% ruthenium–20% platinum containing SiC/C supported RP-121 analog (Pt–Ru/SiC/C) was prepared via a three stage impregnation procedure. Depostion of ruthenium salts was first conducted by evaporation of a 0.03 M ruthenium(III) chloride solution in 15% HCl, followed by reduction of ruthenium to the metal under hydrogen gas at 350°C. This was followed by a two-stage deposition of platinum in which each stage consisted of the sequential addition of 10 aliquots of chloroplatinic acid solution, each containing the mass equivalent of 10% Pt relative to the weight of the support, followed by reduction under hydrogen for 2 h at 350°C.

2.3. SiC/C product characterization

A scintag XDS 2000 powder X-ray diffractometer (XRD) was used to confirm the production of SiC-coated activated carbon, and to identify other crystalline phases present. A JEOL model JSM6300 XV SEM, instrumented with an energy dispersive X-ray spectrometer, was utilized for both imaging and elemental mapping. Carbon was deposited on the surface of non-conductive samples using an Edwards E306A coating system. Elemental analyses were conducted using a CAMECA SX50 electron probe microanalyzer (EPMA). BET surface areas and pore distributions were determined using a Micromeritics Gemini model surface area analyzer. Relative oxidation resistances of the SiC/C product were studied using a DuPont model 951 thermogravimetric analyzer (TGA) and a Mettler model MT5 microbalance.

3. Results and discussion

Six reactor runs were successfully completed. Runs denoted as R1, R2, R3, R4, and R6 utilized activated carbon as the starting material. In R5, P-121, the activated carbon supported bimetallic platinum (20%) — ruthenium (5%) catalyst was used as the carbonaceous reactant. Preliminary experiments indicated that reaction temperatures $\geqslant 1300$°C produced the best results. R-2 was conducted at 1300°C. All other runs utilized reactor temperatures of 1350°C.

All reactor runs yielded products which were significantly different in appearance, as compared to the starting material, both to the naked eye and under examination using a light microscope. The most obvious change was a transition from black to gray coloration. When the perforated gas distributor disk was used, the product removed after completion of the run contained white and reddish brown material thought to be SiO_2 and SiO, respectively. This may have been due to the

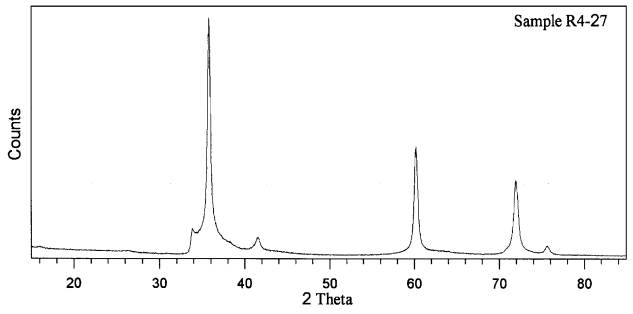

Fig. 3. X-ray diffractogram for silicon-carbide-coated activated carbon sample R4-27. 5 h reaction time at 1350°C with introduction of 1 g SiO at 30 minute intervals.

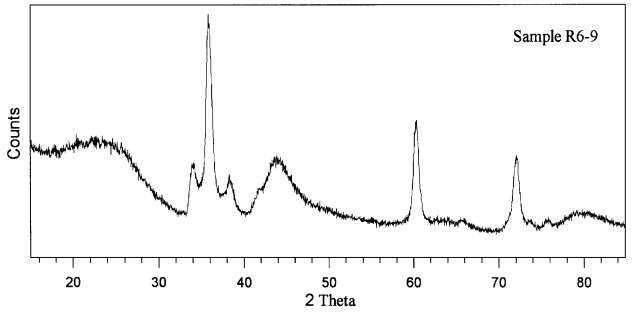

Fig. 4. X-ray diffractogram for silicon-carbide-coated activated carbon: sample R6-9. 8 h reaction time with the introduction of 0.5 g SiO at 30 minute intervals.

creation of a 'dead zone' caused by very few flow channels (perforations) through the ceramic disk. This phenomenon was not observed when the porous distributor was used. The pneumatic introduction of crystalline SiO proved to be the most problematic step in the HTFBR operation. The frequent introduction of small quantities of SiO produced the best results. Future developments should incorporate methods for the continuous introduction of a carefully controlled gaseous SiO feed. Use of higher temperatures should also be considered.

X-ray diffractograms were acquired using representative samples of SiC/C, the carbon-supported platinum–ruthenium catalyst designated as RP-121, and silicon-carbide-coated RP-121. The diffractograms shown in Figs. 3 and 4, for samples R4-27 and R6-9, respectively, are typical of the SiC/C produced by the HTFBR process. (R4-27 indicates the 27th sample collected during Run 4.) The major peaks at 2θ values of 35.5, 60.5, and 72, correspond to β-SiC, the cubic form that is known to predominate at the reaction temperatures used in this investigation. The peak widths at half-peak height are much wider for sample R6-9 as compared to sample R4-27, indicating a smaller crystallite size in R6-9. This suggests that the average crystallite size of the silicon carbide increases over the duration of a coating run.

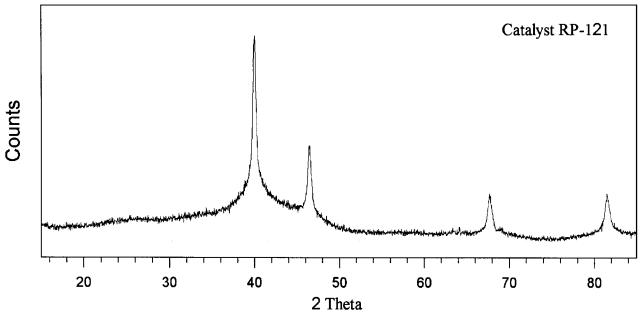

Fig. 5. X-ray diffractogram for untreated RP-121 carbon-supported catalyst.

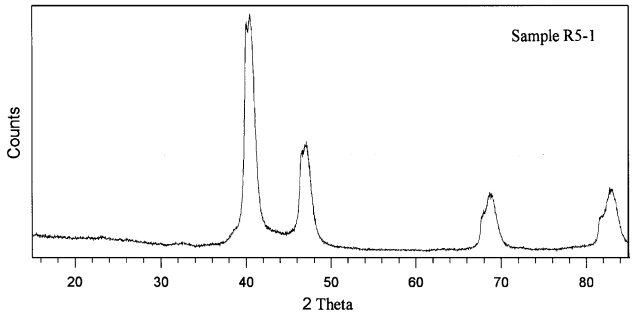

Fig. 6. X-ray diffractogram for RP-121 catalyst treated at 1350°C for 1 h.

The X-ray diffraction pattern for untreated RP-121 catalyst, as shown in Fig. 5, is composed only of peaks corresponding to crystalline platinum. As no shift in the platinum lattice parameters is evident, it can be concluded that a platinum–ruthenium alloy is not present, and that the ruthenium remains amorphous with respect to X-ray diffraction. The highest temperature to which this catalyst is exposed during preparation is 350°C. When the material is heated to 1350°C for 1 h during the pre-treatment stage of the HTFBR coating run, the platinum pattern shifts to the right, which may be due to the inclusion of ruthenium into the platinum lattice. This is seen in the diffractogram for sample R5-1 (Fig. 6). The peaks for the high-temperature pretreated RP-121 are also severely broadened, most likely due to a highly variable composition of the crystallites with respect to ruthenium and platinum content.

As shown in Fig. 7, dramatic changes in the diffraction pattern result when the RP-121 catalyst is exposed to the silicon monoxide at 1350°C to produce the SiC coating. The platinum/ruthenium phase appears to become more homogeneous, as indicated by a narrowing of the peaks, and the elimination of the secondary peaks at lower angles. At higher temperatures, sintering of noble metal catalysts is known to occur, resulting in larger, but less well-dispersed catalytic nuclei. As expected, peaks representing β-SiC are also present. Additionally, the presence of multiple new peaks indicates the creation of at least

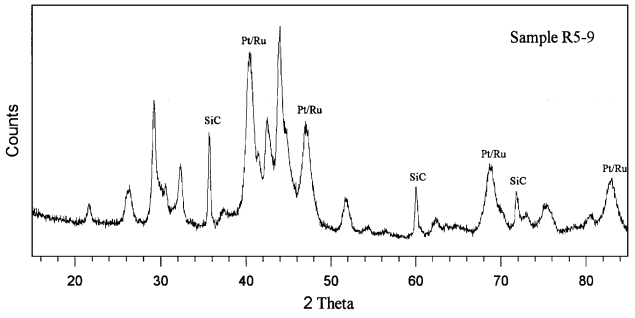

Fig. 7. X-ray diffractogram for SiC-coated RP-121 catalyst. Treated at 1350°C for 8 h with 0.5 g SiO introduction at 30 minute intervals.

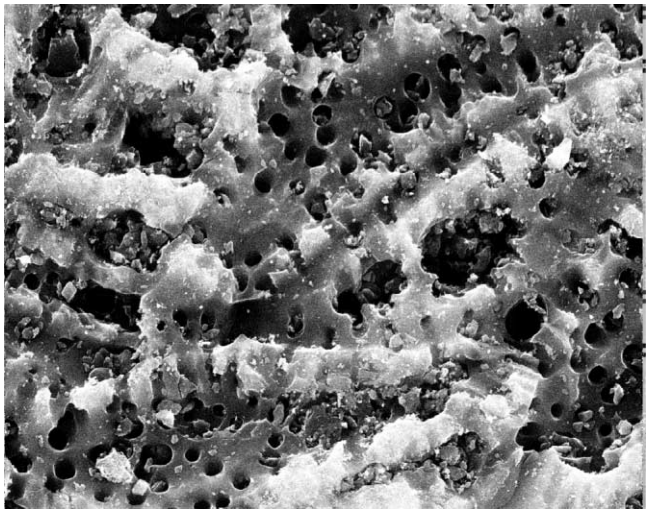

Fig. 8. Scanning electron micrograph — untreated 580-26 activated carbon (2000×).

two new phases. These have not been identified. Possible candidates include: noble metal carbides and silicides.

The morphology of surfaces, interiors of fragments, and the interiors of epoxy mounted and polished samples was examined by scanning electron microscopy. Samples representative of starting materials, intermediate stages of the coating process, and end products were imaged and analyzed. The activated carbon used as the substrate for the RP-121 catalyst and as the carbon source for production of the silicon carbide in the HTFBR process is produced by pyrolysis of coconut shells. This results in a highly irregular surface topography. For this reason, no single image is representative of the carbon surface. However, the image shown in Fig. 8 is typical. The numerous cylindrical holes approximately 1 μm in diameter are thought to represent macropores. However, the vast majority of the surface area corresponds to pores which are less than 50 Å in diameter and are too small to be imaged by SEM.

The conversion of carbon to silicon carbide is evident from the SEM imagery. Silicon carbide is less electrically conductive than the activated carbon substrate. This

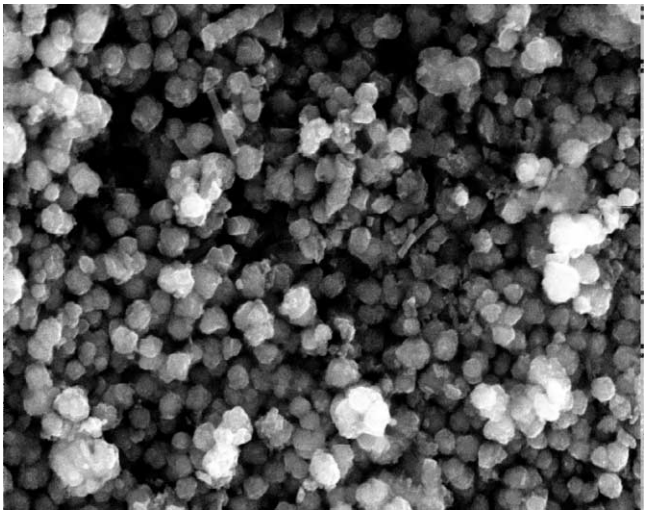

Fig. 9. Scanning electron micrograph of SiC/C — sample R2-20 (8500×).

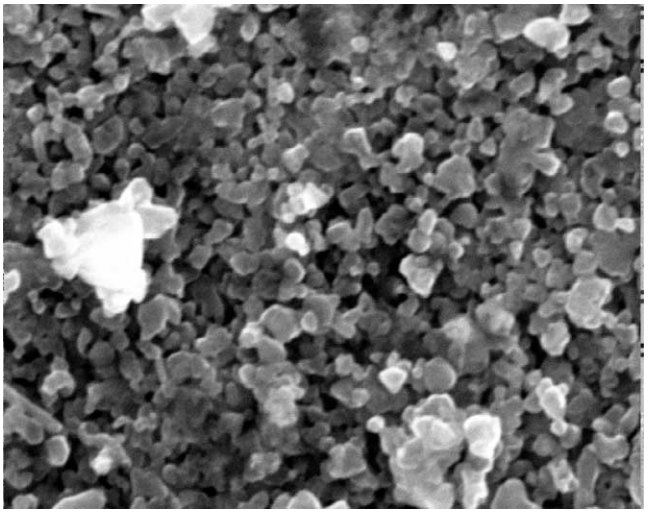

Fig. 10. Scanning electron micrograph of SiC/C — sample R4-27 (20,000×).

results in charging of the sample in SiC-rich localities under the SEM electron bombardment. Consequently, areas composed primarily of silicon carbide appear lighter than regions composed of unreacted carbon. This is evident in the electron micrographs shown in Figs. 9 and 10, which were acquired using final product samples from the fourth and sixth reactor runs, respectively. Both images show the granular growth of silicon carbide which is characteristic of all the silicon-carbide-coated carbon surfaces produced. Grain size is highly variable, but ranges from 0.25 to 1.0 μm, in general. In a significant fraction of samples, small fibers were observed in the deeper crevices of the carbon surface and in internal voids and channels. Structures typical of this fibrous morphology are evident in the two electron micrographs

Fig. 11. Scanning electron micrographs of fibers in sample R4-27. Magnification: 11,000 × -Top, 3700 × -Bottom.

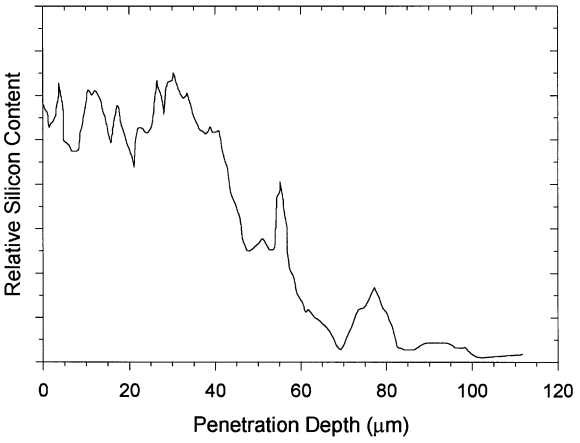

Fig. 12. Silicon distribution in cross-section of a silicon-carbide-coated carbon granule.

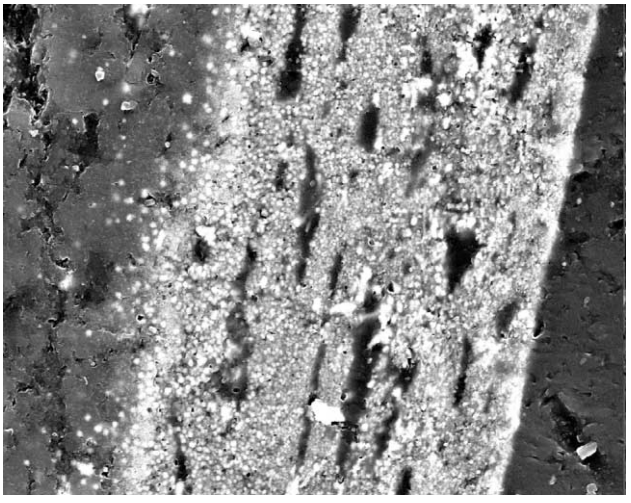

Fig. 13. Scanning electron micrograph of SiC to C transition (1700 ×).

of sample R4-27 presented in Fig. 11. Based upon the reaction chemistry, SiO_2 and SiC were considered the most likely candidates in the formation of these structures. An elemental analysis was conducted by EPMA. The absence of oxygen strongly suggests that these structures are most probably silicon carbide '*whiskers*'. A silicon line scan was performed by X-ray fluorescence spectrometry across the SiC to carbon transition using a cross-section prepared from sample R4-24. The experimental results are presented in Fig. 12. The gradient in silicon content from the outside to the interior of the coated carbon particle is clearly indicated. The SEM image shown in Fig. 13 illustrates a distinct transition from silicon carbide on the right-hand side of the micrograph to unreacted elemental carbon on the left.

For use as a novel catalyst support, the most important properties of the SiC/C product are resistance to chemical attack under reaction conditions, and retention of sufficient surface area and surface affinity characteristics that high-activity catalysts can be prepared. As a comparative means for assessing oxidation resistance, thermogravimetric analyses (TGA) of the activated carbon precursor, the baseline RP-121 carbon-supported catalyst, silicon-carbide-coated RP-121, SiC/C-supported platinum–ruthenium catalyst, and various SiC/C samples were conducted.

Samples were heated under an air flow using a programmed temperature ramp of 10°C/min, from ambient to 800°C to determine the temperatures corresponding to the onset of oxidation, and the relative mass losses between the various materials. The experimental results are shown in Fig. 14. The activated carbon (580-26) was completely oxidized at 500°C. Significantly, both silicon-carbide-coated carbons retained mass throughout the experiment, although the temperatures of onset and the rates of mass loss varied significantly. For RP-121 (R5-1) the mass remaining at 800°C corresponds to the noble

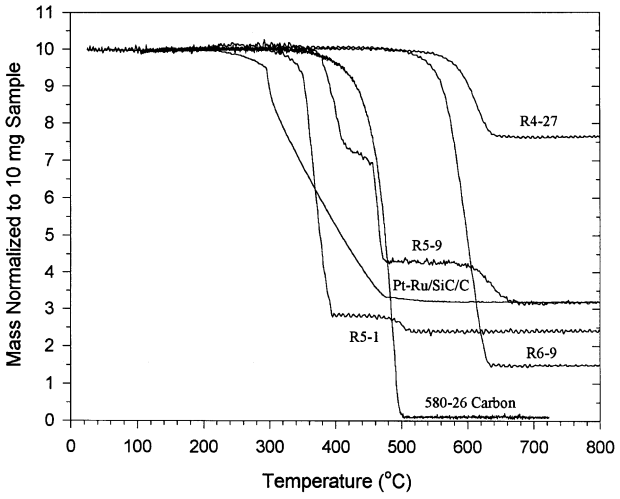

Fig. 14. TGA results from ambient temperature to 800°C at 10°C/min.

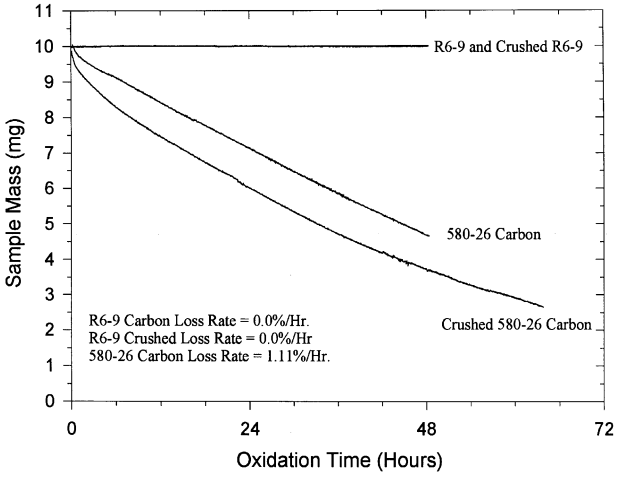

Fig. 15. Isothermal TGA of SiC/C and 580-26 activated carbon substrate at 245°C.

metal content, indicating complete decomposition of the carbon support. Stepwise changes in the oxidation rate were observed with increasing temperature in both the untreated and the silicon-carbide-coated RP-121 catalyst. For the silicon-carbide-coated Pt–Ru-bearing catalysts (R5-9, and R6-9), retention of mass in excess of the noble metal content was evident. Given that these catalysts contained an initial noble metal content of $\approx 25\%$, the remaining mass indicates the presence of a significant SiC (or protected carbon) content. It is also apparent that the RP-121 carbon-supported catalyst (R5-1) is less stable with respect to oxidation than the 580-26 activated carbon support. This is not surprising in view of the fact that RP-121 is an extremely active and non-selective oxidation catalyst.

Isothermal TGA was performed at 245°C on samples of the 580-26 carbon substrate and the silicon-carbide-coated sample R6-9 under an air flow. Samples of each were also crushed to a fine powder and then analyzed under identical conditions. The resulting mass losses are presented in Fig. 15 as functions of oxidation time. Both the granular and the powdered 580-26 activated carbon exhibited significant losses due to oxidation, with loss rates of approximately 1% h^{-1}. No mass loss was observed under these conditions for either the granular or the powdered SiC/C material. The resistance to oxidation in the crushed SiC/C indicates that the formation of silicon carbide penetrates the interior of the porous network sufficiently to provide a substantial barrier against the diffusion of oxygen to a reactive carbon site. Similar experiments were performed using the RP-121, silicon-carbide-coated RP-121, and the SiC/C-supported Pt–Ru catalyst. These isothermal TGA results are presented in Fig. 16.

BET surface areas were determined for the 580-26 activated carbon substrate and for numerous samples in

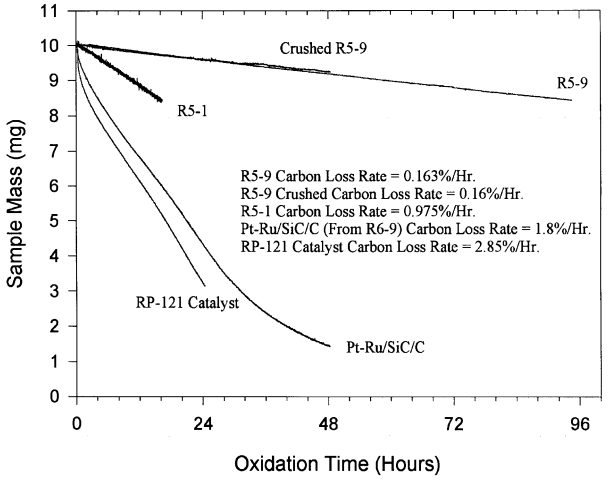

Fig. 16. Isothermal TGA of catalysts at 245°C.

various stages of the silicon-carbide-coating process, corresponding to reactor runs 2, 4, 5, and 6. These data are summarized in Table 1. The samples were then oxidized in air at 800°C for 2 h to achieve the complete oxidation of elemental carbon to CO_2. The results of these experiments are presented in Fig. 17. In the case of samples from runs 2, 4, and 6, the remaining mass can be attributed to SiC (and possibly to carbon which is protected from oxidation). These results indicate an approximately linear inverse relationship between the BET surface area and % conversion to silicon carbide. This suggests that a silicon-carbide-coated carbon product can be prepared to yield a given surface area or degree of robustness by careful control of the extent of SiC formation, and also that the production of SiC/C catalyst supports are possible which embody optimal tradeoffs between surface area and resistance to chemical attack.

Table 1
Summary of BET surface areas. Samples are designated by run (R) number and sequential order of sampling. The -800 suffix identifies samples oxidized at 800°C for 2 h

Sample ID	Surface area (m^2/g)	Sample ID	Surface area (m^2/g)	Sample ID	Surface area (m^2/g)
R1-9	1168	R5-3	1126	R6-7	1416
R2-8	1173	R5-4	1042	R6-8	1374
R2-19	150	R5-5	984	R6-9	1263
R2-20	134	R5-6	983		
R4-9	1273	R5-7	1000	RP-121	1323
R4-13	1048	R5-8	916	580-26	1756
R4-17	740	R5-9	892		
R4-22	559	R6-2	1568	R2-19-800	8.3
R4-26	408	R6-3	1528	R2-20-800	10.3
R4-27	402	R6-4	1458	R4-25-800	6.7
R5-1	1261	R6-5	1457	R4-26-800	6.3
R5-2	1209	R6-6	1448	R4-27-800	6.3

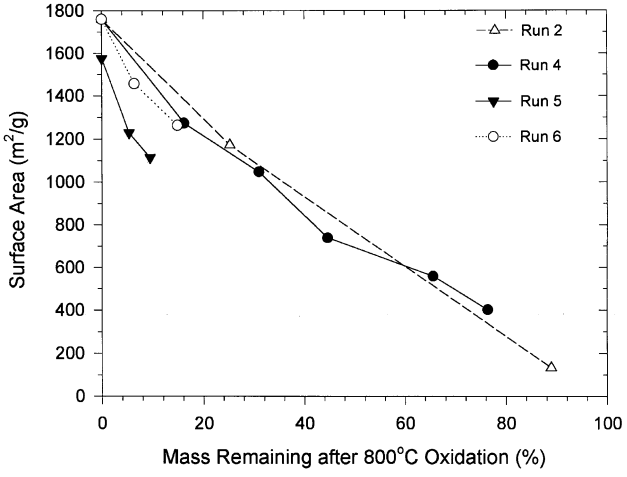

Fig. 17. BET surface area versus oxidation resistance resulting from SiC formation.

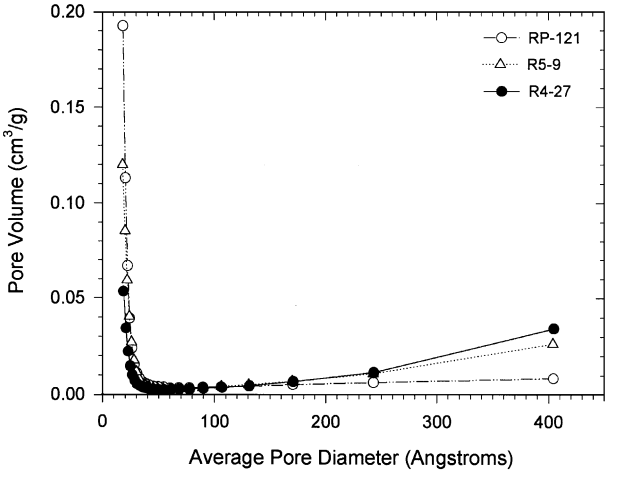

Fig. 18. Pore size distributions.

Pore size distributions were also characterized for RP-121, silicon-carbide-coated RP-121 (R5-9), and a typical SiC/C (R4-27) covering pore diameters ranging between 20 and 400 Å. These are illustrated in Fig. 18. When the carbon in the RP-121 catalyst undergoes conversion to silicon carbide, a significant portion of the smaller pore volume is lost, while the larger diameter pore volume is more than doubled. However, because the smaller pores provide a higher surface area to volume ratio a net loss in surface area occurs. The loss of small pores is also evident in the SiC/C sample, but with a modest increase in the larger pores.

4. Conclusions

The feasibility of producing a SiC/C using the high-temperature fluidized-bed-reactor-based process has been conclusively demonstrated. The resulting materials have been shown to exhibit improved resistances to thermal and chemical decomposition, while retaining sufficient surface area and surface affinity to function as supports for high-activity noble metal catalysts. The formation of β-SiC crystallites on the carbon surface during the coating process was confirmed by X-ray diffractometry. Scanning electron microscopy, in conjunction with electron probe microanalysis, indicated the formation of structures believed to represent silicon carbide whiskers within the porous network, in addition to the formation of crystallites and crystalline layers at the surface. Both the degree of resistance to oxidation and the surface area of the SiC/C product were found to vary in inverse proportion to the extent of conversion of carbon to silicon carbide. Thus, in the future, it should be possible to determine the optimal trade-off between surface area and robustness to provide high levels of performance as a catalyst support.

The Pt–Ru catalysts utilized in this study are unusual in their extremely high levels of non-specific activity toward oxidation. When prepared using carbonaceous materials these catalysts literally promote the decomposition of their support matrices. Thus, the support materials used in the preparation of these catalysts were exposed to a 'worst-case scenario' with respect to the rigor of chemical attack. However, most commercial catalysts are both far less active and far more specific in the reactions which they promote. For this reason they are less likely to facilitate decomposition of the support. Thus, the gains in resistance to thermal and chemical degradation exhibited for the Pt–Ru/SiC/C catalyst in comparison to the untreated RP-121 may be substantially greater when applied to the preparation of more conventional catalysts.

Because the optimal trade-off between remnant surface area and silicon carbide formation may occur at different points for different applications, future work should include the identification of the important variables in reactor operation which can be manipulated to produce products of varying composition, and also on the development of methods to control the process so that products of uniform and carefully controlled properties can be prepared. Based upon experience gained in this initial effort, the most obvious improvement required for better control of product composition and uniformity, is the development of means for the continuous introduction of SiO gas into the fluidized bed. This may be achieved using the reaction between elemental silicon and SiO_2 at high temperature, in a separate upstream reactor. The use of higher reactor temperatures may also be of benefit.

Acknowledgements

This material is based upon work supported by the National Science Foundation under award no. DMI-9760204.

References

Akse, J. R., Atwater, J. E., McKinnis, J. A., Thompson, J. O., & Hurley, J. A. (1997). Elimination of organic contaminants in wastewater using molecular oxygen and the aqueous phase catalytic oxidation process. *Seventh international chemical oxidation symposium*, Nashville, TN, April 9–11.

Akse, J. R., & Jolly, C. D. (1991). Catalytic oxidation for treatment of ECLSS & PMMS waste streams. In A. Behren, R. D. MacElroy, & R. P. Reysa (Eds.), *Regenerative life support systems and processes*. Warrendale, PA: Society of Automotive Engineers.

Akse, J. R., Thompson, J. O., Scott, B., Jolly, C., & Carter, D. L. (1992). Catalytic oxidation for treatment of ECLSS & PMMS waste streams. *SAE Transactions, Journal of Aerospace*, *101*, 910–925.

Atwater, J. E., Akse, J. R., McKinnis, J. A., & Thompson, J. O. (1996). Aqueous phase heterogeneous catalytic oxidation of trichloroethylene. *Applied Catalysis B: Environmental*, *11*(1), L11–L18.

Atwater, J. E., Akse, J. R., McKinnis, J. A., & Thompson, J. O. (1997a). Low temperature aqueous phase catalytic oxidation of phenol. *Chemosphere*, *34*, 203–212.

Atwater, J. E., Akse, J. R., Rodarte, J. M., Thompson, J. O., Wang, T.-C., & Hurley, J. A. (1997b). Silicon carbide coated granular activated carbon: A robust support for low temperature aqueous phase oxidation catalysts. *Carbon*, *35*(10–11), 1678–1679.

Bruno, C., Walsh, P. M., Santavicca, D. A., Sinha, N., Yaw, Y., & Bracco, F. V. (1983). Catalytic combustion of propane/air mixtures on platinum. *Combustion Science & Technology*, *31*, 43–74.

Cuong, P. H., Main, S., Ledoux, M., Weibel, M., Ehret, G., & Benaissa, M. (1994). Synthesis and characterization of platinum-rhodium supported on SiC and SiC doped with cerium: Catalytic activity for the automobile exhaust reaction. *Applied Catalysis B: Environmental, 4,* 45–63.

Jovanovic, Z., Kimura, S., & Levenspiel, O. (1994). Effect of hydrogen and temperature on the kinetics of the fluidized-bed nitridation of silicon. *Journal of the American Ceramic Society*, *77*(1), 186–192.

Kage, H., Yoshida, T., Ogura, H., & Matsuno, Y. (1996). Coating efficiency of seed particles in a fluidized bed by atomization of a powder suspension. *Powder Technology*, *86*, 243.

Kunii, D., & Levenspiel, O. (1991). *Fluidization engineering* (2nd ed.). Boston: Butterworth-Heinemann.

Ledoux, M., Guille, J., Hantzer, S., & Dubots, D. (1990). *Process for the production of silicon carbide with a large specific surface area and use for high-temperature catalytic reactions*, U.S. Patent No. 4,914,070.

Ledoux, M., Hantzer, S., Cuong, P. H., Guille, J., & Desaneaux, M. P. (1988). New synthesis and uses of high-specific-surface SiC as a catalytic support that is chemically inert and has high thermal resistance. *Journal of Catalysis*, *114*, 176.

Levenspiel, O. (1972). *Chemical reaction engineering* (2nd ed.). New York: Wiley.

Moene, R., Kramer, L. F., Schoonman, J., Makkee, M., & Moulijn, J. A. (1997). Synthesis of high surface area silicon carbide by fluidized bed chemical vapor deposition. *Applied Catalysis A: General*, *162*, 181–191.

Moene, R., Makkee, M., & Moulijn, J. A. (1998). High surface area silicon carbide as catalyst support characterization and stability. *Applied Catalysis A: General*, *167*, 321–330.

Morooka, S., Okubo, T., & Kusakabe, K. (1990). Recent work on fluidized bed processing of fine particles as advanced materials. *Powder Technology*, *63*, 105.

Parmaliana, A., Alekseev, O. S., Nesterov, G. A., Ryndin, Y. A., & Giordano, N. (1986). Dispersity effect of platinum supported on honeycomb carrier its activity in benzene hydrogenation. *Reaction Kinetics & Catalysis Letters*, *32*, 199–204.

Sharma, R. K., Zhou, B., Tong, S., & Chuang, K. T. (1995). Catalytic destruction of volatile organic compounds using supported platinum and palladium hydrophobic catalysts. *Industrial Engineering Chemistry Research*, *34*, 4310–4317.